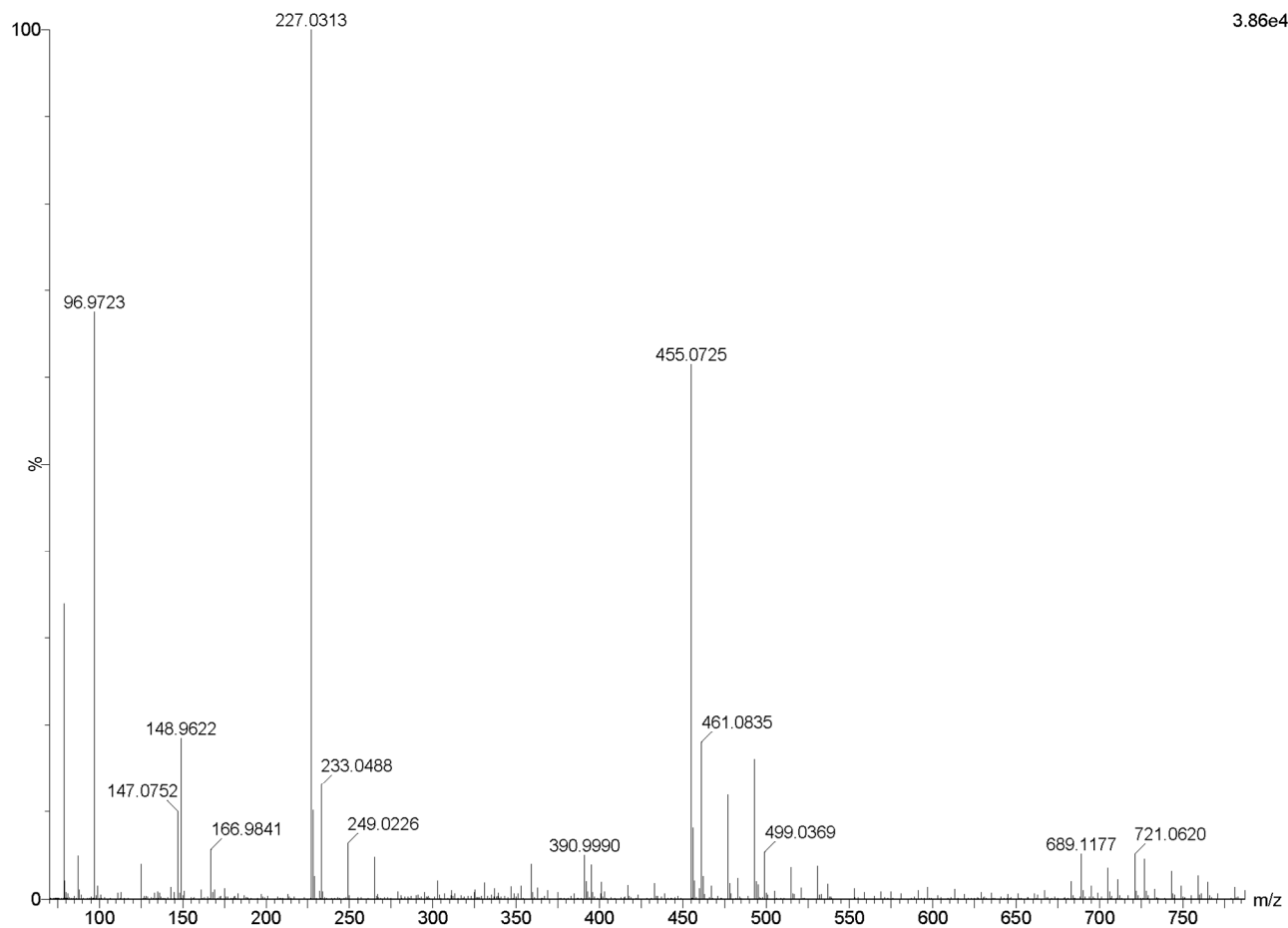
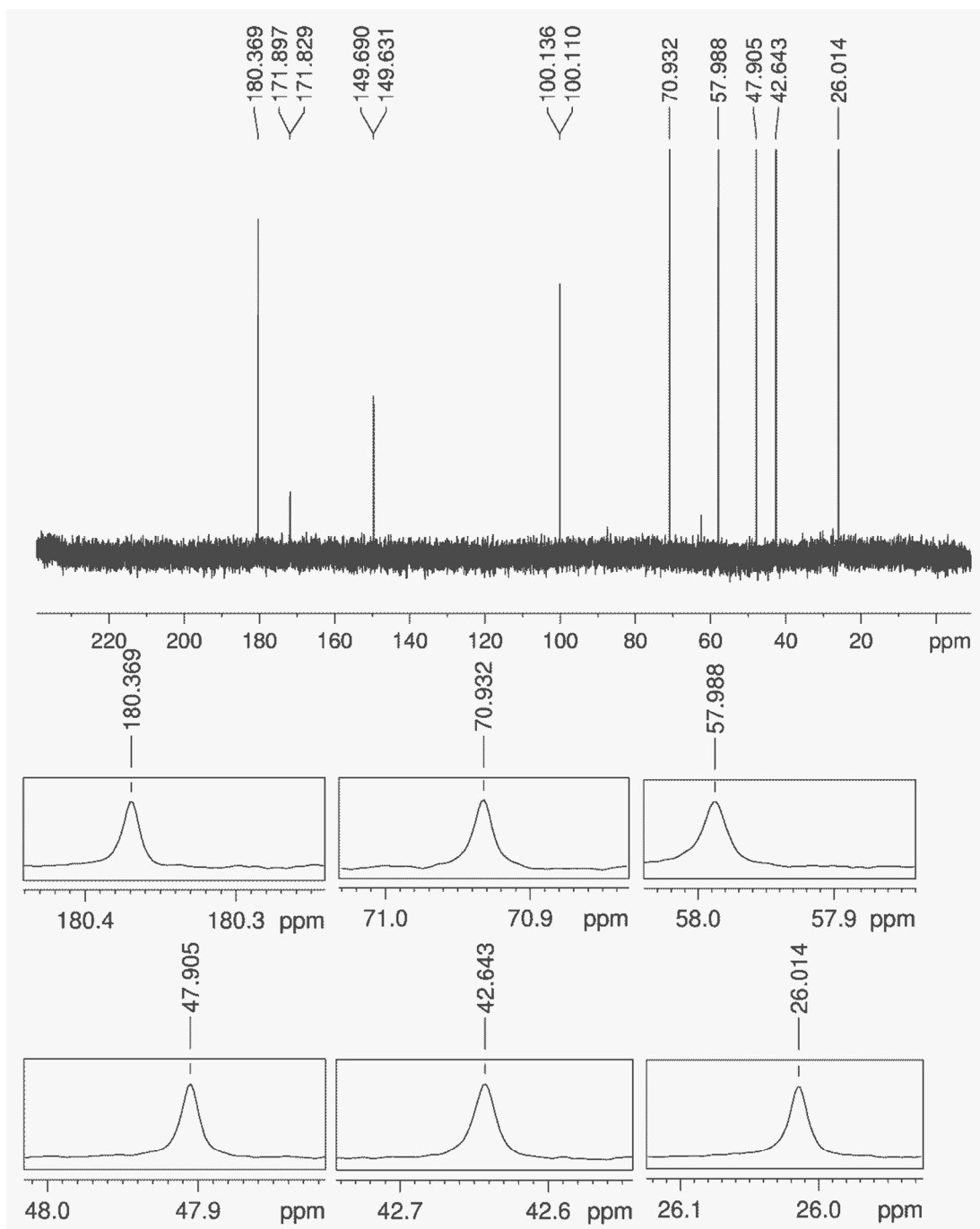


**SUPPLEMENTAL INFORMATION**  
*A Novel Mevalonate Pathway in Archaea*  
J. Vinokur, T.P. Korman, Z. Cao, J.U. Bowie.



**Figure S1.** Electrospray ionization mass spectrum after Ta1305 activity with (*R*)-Mevalonate, collected with a Waters LCT Premier XE time of flight instrument. A sample directly from the NMR experiment was transferred to a GC vial and injected into the multi-mode ionization source with a Waters Acquity UPLC. We observed a mass of 227.0313 m/z which is within 0.00008 m/z of the mass expected for a phosphorylated mevalonate [ $C_6H_{13}O_7P - H$ ].



**Figure S2.** Full  $^{13}\text{C}$  NMR spectrum of the no enzyme control from figure 3A. Six single peaks corresponding to the six carbons of unreacted mevalonate are shown in the inserts. The additional three peaks between 100 ppm and 175 ppm are from phosphoenolpyruvate, included in the reaction to regenerate ATP and simplify the spectrum. Spectra were acquired at ambient temperature on a 500 MHz Bruker AV500 spectrometer equipped with a cryoprobe.

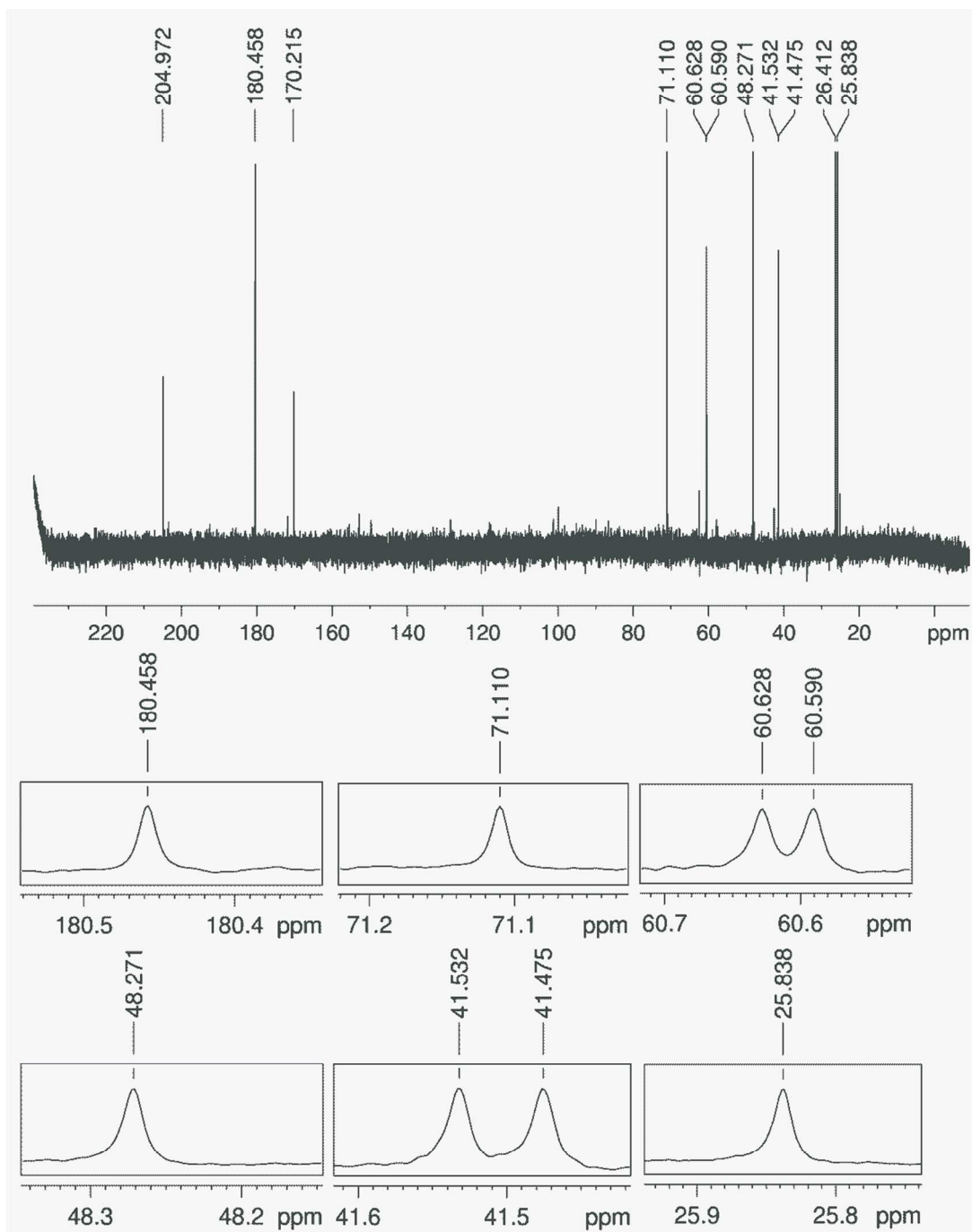


**Figure S3.** Full  $^{13}\text{C}$  NMR spectrum of yeast mevalonate-5-kinase activity on (*R*)-Mevalonate from figure 3B. Six chemical shifts corresponding to the six carbons of mevalonate-5-phosphate are shown in the inserts. The additional three peaks at 204.972, 170.215, and 26.412 ppm are from 10 mM pyruvate, which is made during the regeneration of ATP. Spectra were acquired at ambient temperature on a 500 MHz Bruker AV500 spectrometer equipped with a cryoprobe.

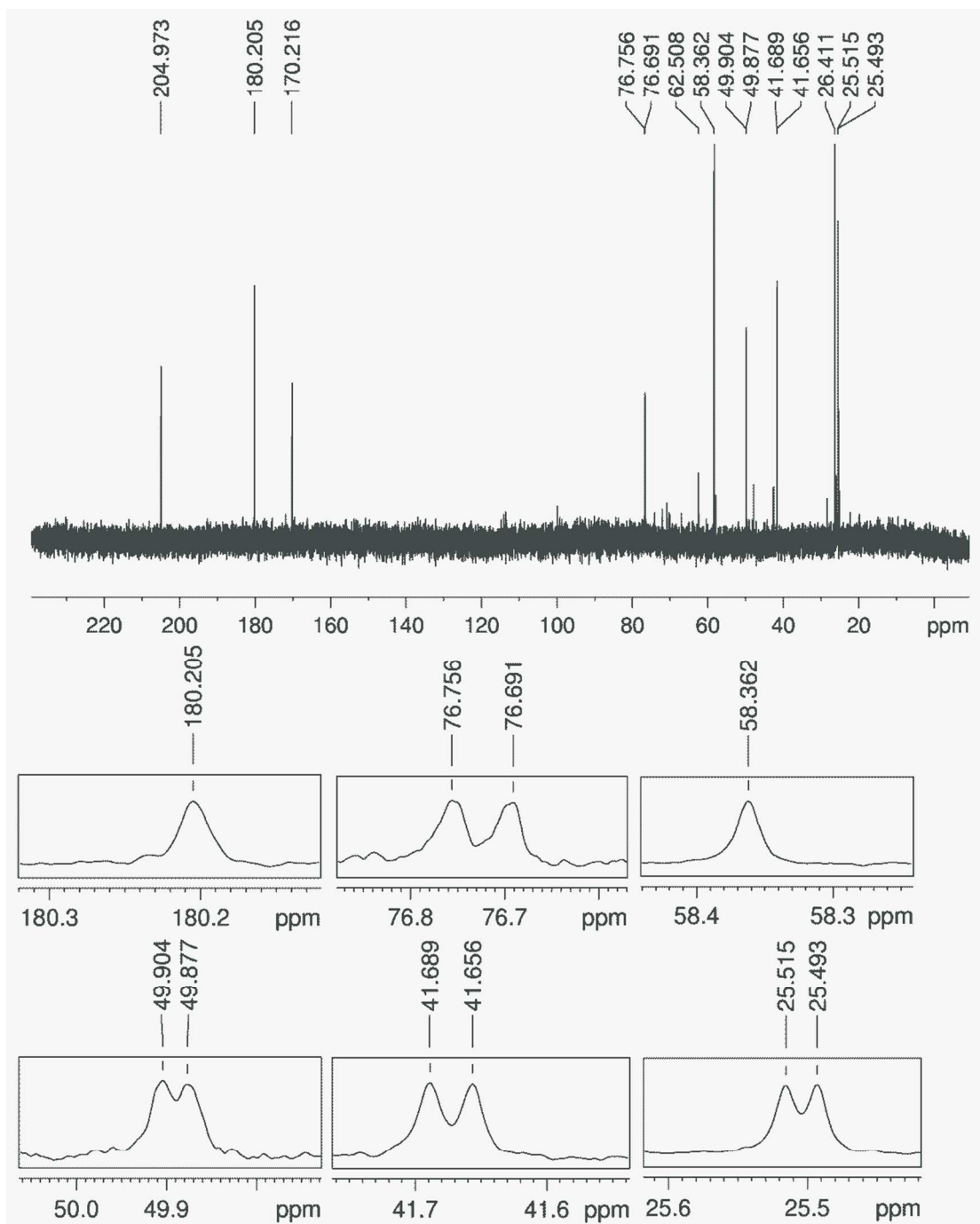


**Figure S4.** Full  $^{13}\text{C}$  NMR spectrum of mevalonate-3-kinase (Ta1305) activity on (*R*)-Mevalonate from figure 3C. Six chemical shifts corresponding to the six carbons of mevalonate-3-phosphate are shown in the inserts. The additional three peaks at 204.973, 170.216, and 26.411 ppm are from 10 mM pyruvate, which is made during the regeneration of ATP. Spectra were acquired at ambient temperature on a 500 MHz Bruker AV500 spectrometer equipped with a cryoprobe.

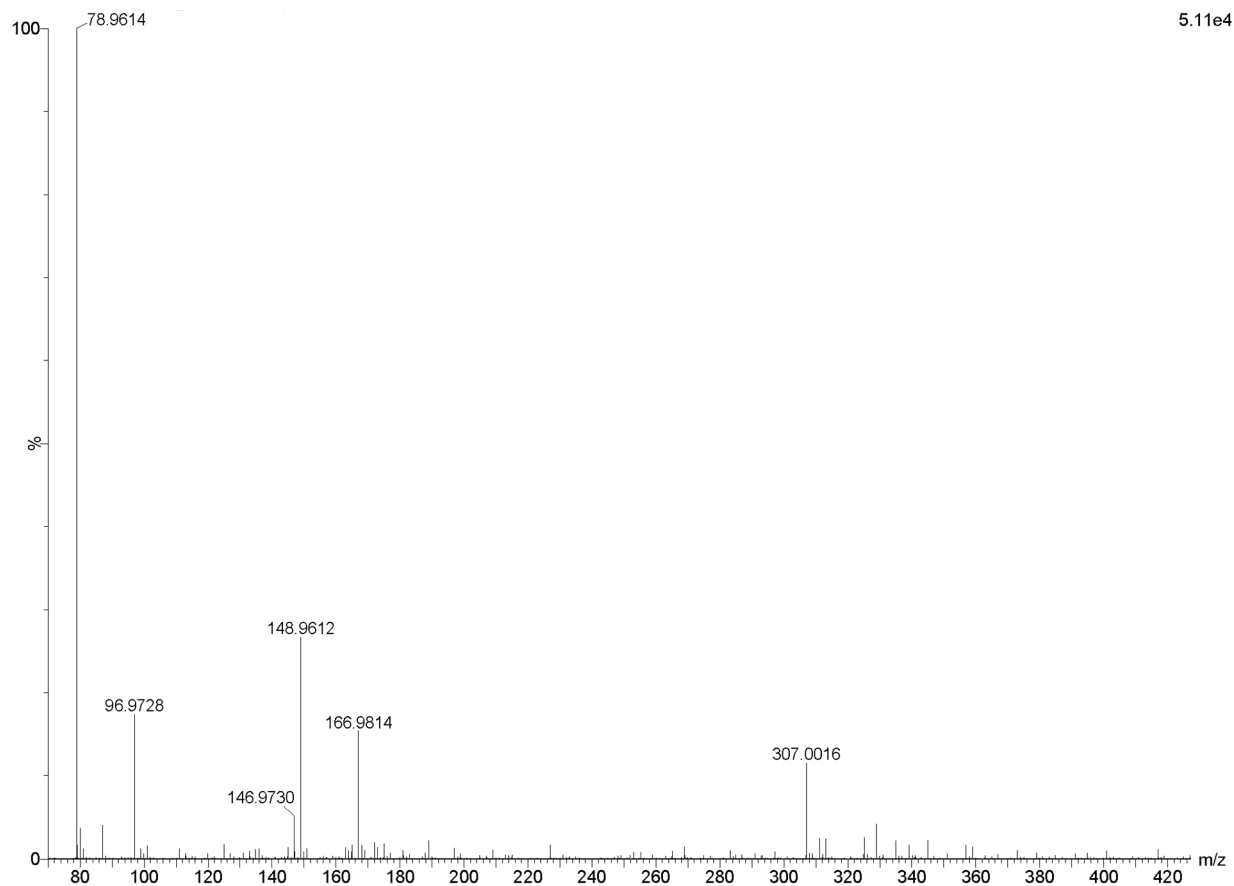


**Figure S5.** Negative electrospray ionization mass spectrum after Ta0762 and Ta1305 activity with (*R*)-Mevalonate was collected with a Waters LCT Premier XE time of flight instrument. A sample directly from the NMR experiment was transferred to a GC vial and injected into the multi-mode ionization source with a Waters Acquity UPLC. We observed a mass of 307.0016 *m/z* which is within 0.0031 *m/z* of the mass expected for mevalonate diphosphate [ $C_6H_{14}O_{10}P_2 - H$ ]<sup>-</sup>

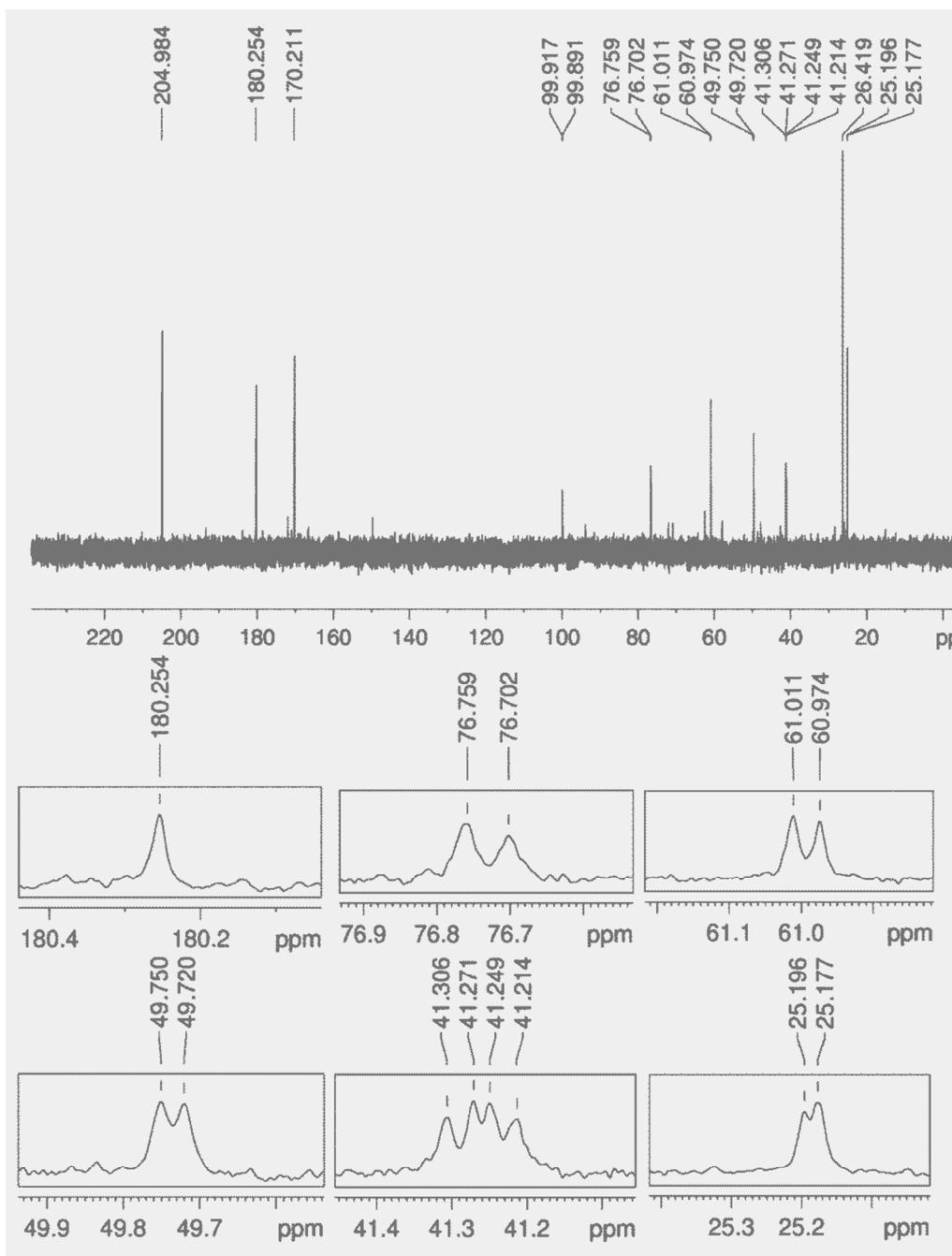


**Figure S6.** Full  $^{13}\text{C}$  NMR spectrum of mevalonate-3-kinase (Ta1305) and mevalonate-3-phosphate-5-kinase (Ta0762) activity on (*R*)-Mevalonate from figure 3D. Six chemical shifts corresponding to the six carbons of mevalonate-3,5-bisphosphate are shown in the inserts. The additional three peaks at 204.984, 170.211, and 26.419 ppm are from 10 mM pyruvate, and the doublet at 99.904 is from unreacted PEP. Spectra were acquired at ambient temperature on a 500 MHz Bruker AV500 spectrometer equipped with a cryoprobe.

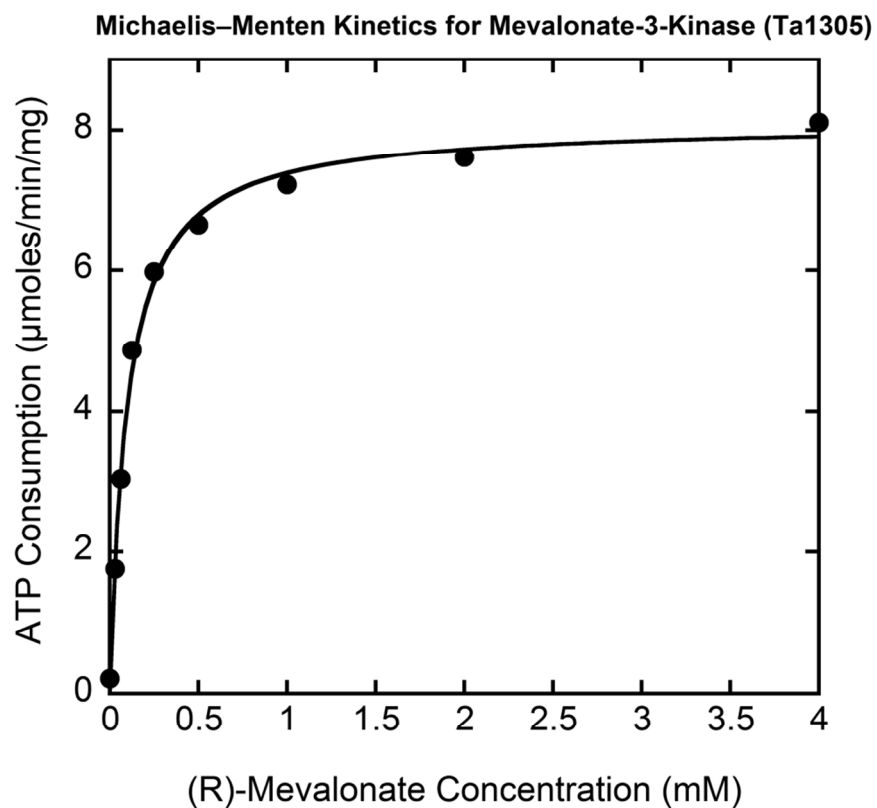


**Figure S7.** Michaelis-Menton plot for mevalonate-3-kinase (Ta1305). The enzyme was found to have a  $k_m$  of  $97 \pm 6 \mu\text{M}$  and  $k_{\text{cat}}$  of  $5.0 \pm 0.1 \text{ s}^{-1}$  with respect to (*R*)-Mevalonate, which is comparable to mevalonate-5-kinase from another archeon, *Methanosarcina mazei* ( $k_m$  of  $68 \pm 4 \mu\text{M}$ ,  $k_{\text{cat}}$  of  $4.3 \pm 0.2 \text{ s}^{-1}$ ) (25). Kinetic data was analyzed using Kaleidagraph 4.1 (Synergy Software).

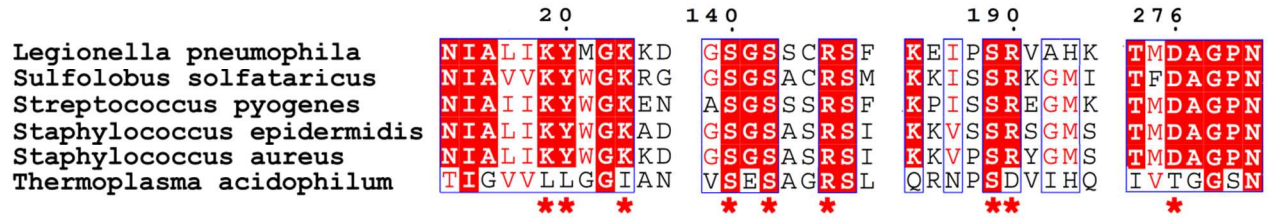


**Figure S8.** Clustal Omega sequence alignment of five bacterial mevalonate pyrophosphate decarboxylases (MDCs) with mevalonate-3-kinase from *T. acidophilum*. Red stars indicate active site residue that interact with mevalonate pyrophosphate in a MDC crystal structure by Barta *et al.* (33). Red highlighting indicated that at least 5 of 6 amino acids are identical. Only 4 out of 9 active site residues are conserved in mevalonate-3-kinase, suggesting that L19, L12, I23, D190, or T276 may be responsible for the loss of decarboxylase activity.